Journal of the Physical Society of Japan **82** (2013) 124711 **FULL PAPERS**
http://dx.doi.org/10.7566/JPSJ.82.124711

Magnetic Properties of Layered Itinerant Electron Ferromagnet Fe_3GeTe_2

Bin CHEN[1,2*], JinHu YANG[1], HangDong WANG[1], Masaki IMAI[2], Hiroto OHTA[2], Chishiro MICHIOKA[2], Kazuyoshi YOSHIMURA[2†], and MingHu FANG[3]

[1]*Department of Physics, Hangzhou Normal University, Hangzhou 310036, China*
[2]*Department of Chemistry, Graduate School of Science, Kyoto University, Kyoto 606-8502, Japan*
[3]*Department of Physics, ZheJiang University, Hangzhou 310018, China*

(Received July 24, 2013; accepted September 24, 2013; published online November 13, 2013)

We have successfully synthesized a single-crystal sample of the layered structure ferromagnet Fe_3GeTe_2 and present the results of its complete characterization using powder X-ray diffraction (XRD), magnetic susceptibility $\chi(T)$, isotherm magnetization $M(H)$, specific heat $C(T)$, and electrical resistivity $\rho(T)$ measurements. The rietveld refinement of the powder XRD data confirms that Fe_3GeTe_2 crystallizes in the space group $p6_3/mmc$. The $\chi(T)$, $C(T)$, and $\rho(T)$ data indicate bulk ferromagnetic ordering at $T_C = 220$ K with a saturation moment of 1.625 μ_B/Fe at zero temperature. The magnetic measurements of the external magnetic field H applied along the c-axis and ab-plane show a large anisotropy in this material. We found that the modified Arrott plot (M^4–H/M) rather than the M^2–H/M plot is obeyed in this material. The generalized Rhodes–Wohlfarth ratio indicates an itinerant magnetism in this material. The spin fluctuation parameters are estimated and the magnetic properties are discussed in the framework of the self-consistent renormalization (SCR) and Takahashi theory of spin fluctuations.

KEYWORDS: Fe_3GeTe_2, itinerant ferromagnet, SCR, Arrott plot

1. Introduction

The theoretical and experimental studies of itinerant magnetic materials with layered crystal structure in the frame of the self-consistent renormalization (SCR) theory of spin fluctuations can be traced back to the the discovery of cuprate superconductors whose mother compound has two-dimensional characteristics. Compared with Moriya who developed the SCR theory of spin fluctuations for the purely two-dimensional (2D) magnetic system,[1)] Takahashi expanded the SCR theory to the quasi-two-dimensional magnetic system by assuming that the sum of zero-point and thermal spin fluctuations against temperature is nearly conserved.[2)] Ikeda et al. performed a quantitative comparison between the theoretical and experimental results in the $Sr_{1-x}Ca_xRu_2O_7$ system,[3)] and pointed out the possibility of the appearance of quasi-2D weak ferromagnetism in this system on the basis of magnetic measurements. Recently, owing to the discovery of iron-pnictide superconductors, much attention has been paid to the electronic states in 2D magnetic materials, such as the weak itinerant ferromagnets LaCoAsO[4–6)] and LaCoPO,[6–8)] which have the same crystal structure as LaFeAsO.[9)] Magnetic and nuclear magnetic resonance measurements indicate that 2D spin fluctuations play an important role in these materials, and the magnetic properties were discussed in the framework of the SCR theory. However, the quantitative comparison between the theoretical and experimental results is quite rare, particularly for the magnetic materials with relatively higher Cruie temperature.

Fe_3GeTe_2 is a ternary compound that was first synthesized by Abrikosov et al.[10)] Magnetic measurements show that it is an itinerant ferromagnet with a Curie temperature $T_C =$ 230 K.[11)] The X-ray diffraction (XRD) result indicates that it has a hexagonal crystal structure with the space group $p6_3/mmc$, as shown in Fig. 1. Its most pronounced character is the layered Fe_3Ge substructure sandwiched by two layers of Te atoms and a van der Waals gap between adjacent

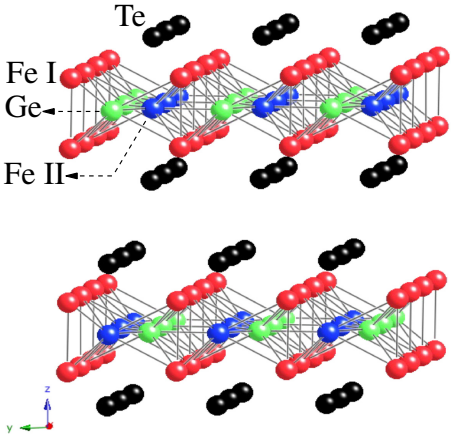

Fig. 1. (Color online) Crystal structure of Fe_3GeTe_2.

Te layers.[11)] Hence, it may be a rare example with a ferromagnetic order in the Fe–Ge–Te system to the best of our knowledge. Anisotropic magnetic properties are strongly expected in this material. In other words, Fe_3GeTe_2 provides a good opportunity to perform a quantitative study of the magnetic properties of a quasi-2D itinerant magnetic material.

In this study, we investigate high-quality single-crystal samples of Fe_3GeTe_2 by electrical resistivity, specific heat, magnetic susceptibility, and isotherm magnetization measurements in detail. The measurements of the magnetic properties with an external magnetic field applied in the ab-plane and along the c-axis indicate that the magnetic properties of this compound show a high anisotropic. Usually, the use of Arrott plots (M^2–H/M) is the standard method of determining the Curie temperature T_C. However, our results suggest that the modified Arrott plot (M^4–H/M) rather than the M^2–H/M plot is obeyed in this compound. T_C is determined to be 220 K for Fe_3GeTe_2 using the modified Arrott plot and electronic resistivity and heat

capacity measurements. Through the quantitative analysis performed on the basis of the Takahashi theory of spin fluctuations, we successfully reproduce the reciprocal magnetic susceptibility above T_C. Our results indicate that Fe_3GeTe_2 is a quasi-2D itinerant ferromagnet.

2. Experimental Procedure

We prepared single-crystal samples of Fe_3GeTe_2 by the chemical transport method with iodine as the transport agent. High-purity Fe (99.99%), Ge (99.999%), and Te (99.995%) were obtained in a stoichiometric molar ratio of 3 : 1 : 2. All of them were placed in an evacuated quartz tube together with 2 mg/cm^3 iodine. Then, we set up the quartz tube in a temperature gradient of 750/700 °C for one week. Single crystals with a tabular shape in the *ab*-plane were grown on the low-temperature side. The dimensions of a typical sample are $2 \times 2 \times 0.25\,mm^3$. We determined the molar ratio of the Fe, Ge, and Te concentrations as 3 : 1.02 : 1.98 by energy-dispersive X-ray spectroscopy, which is almost consistent with the nominal molar ratio. The phase purity of the sample was examined by powder XRD analysis using Cu Kα radiation.

The magnetization M and the magnetic susceptibility $\chi(T) = M/H$, where H is the applied magnetic field, were measured in the temperature range of $2 \leq T \leq 350\,K$ on a single-crystal sample ($2.5 \times 2.5 \times 0.2\,mm^3$, 3.0 mg) in a commercial Quantum Design superconducting quantum interference device magnetometer. The dc resistivity $\rho(T)$ was measured using a standard four-probe technique by applying a current of 5 mA, and the heat capacity $C_P(T)$ was measured under zero magnetic field. Both $\rho(T)$ and $C_P(T)$ measurements were performed using a Quantum Design physical property measurement system. The same crystals were used for these measurements.

3. Results and Discussion

3.1 XRD measurements

The phase purity of the powdered single-crystal samples was determined using a Rigaku Geigerflex powder X-ray diffractometer with Cu Kα radiation ($\lambda_{av} = 1.54182$ Å). Rietveld refinements of the data were carried out using the GSAS package.[12,13] Figure 2 shows the Rietveld refinement fit to the X-ray powder diffraction pattern of Fe_3GeTe_2. All the peaks could be indexed and fitted very well on the basis of the hexagonal crystal structure with the $p6_3/mmc$ space group. The refinement reveals the single-phase nature of the sample without any impurity phase. The obtained lattice parameters are $a = 4.0299$ Å and $c = 16.3425$ Å. These values are very close to the reported ones ($a = 3.991$ Å and $c = 16.333$ Å).[11]

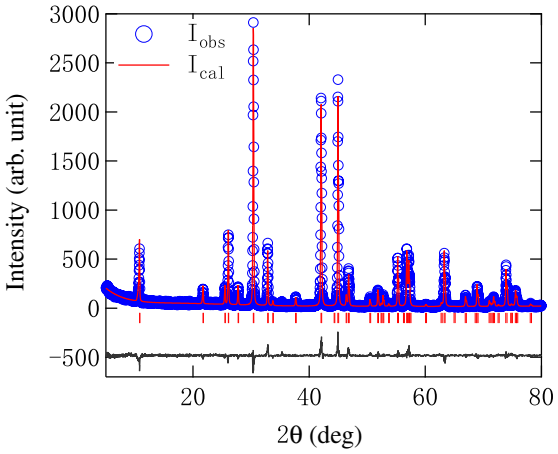

Fig. 2. (Color online) X-ray powder diffraction pattern (open circles) measured at room temperature for Fe_3GeTe_2. The solid line represents the Rietveld refinement fit with the $p6_3/mmc$ space group.

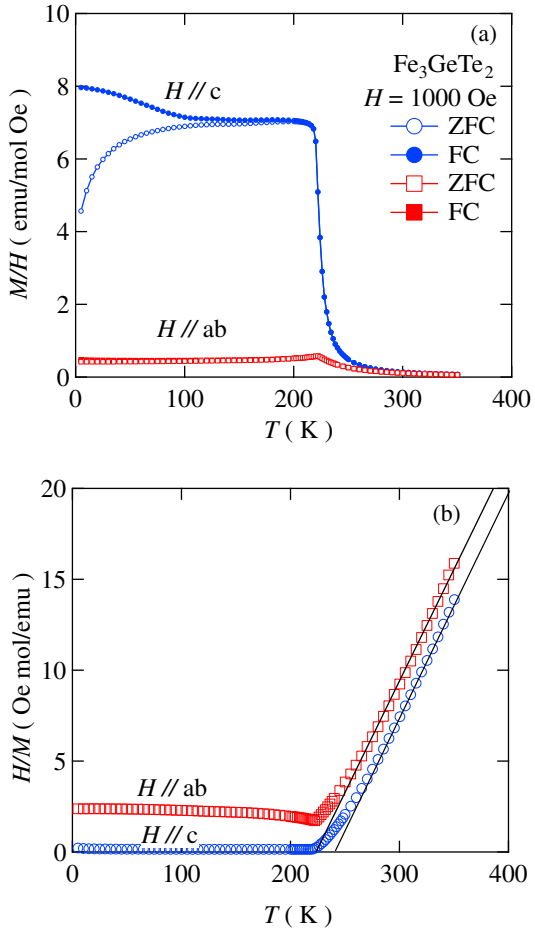

Fig. 3. (Color online) (a) Temperature dependence of magnetic susceptibilities of Fe_3GeTe_2 measured from 2 to 350 K with the external magnetic field ($H = 1000$ Oe) applied along the *c*-axis and in the *ab*-plane. (b) Temperature dependence of inverse magnetic susceptibilities for Fe_3GeTe_2. The solid lines indicate the fit with the modified Cruie–Weiss law.

3.2 Magnetic measurements

Figure 3(a) shows the temperature dependence of the magnetic susceptibility $\chi(T)$ for Fe_3GeTe_2 measured with H (= 1000 Oe) applied parallel to the crystallographic *c*-axis and *ab*-plane, respectively. A rapid increase in $\chi(T)$ for $H \parallel ab$ and $H \parallel c$ at about 220 K suggests the magnetic phase transition at this temperature. The zero-field-cool (ZFC) and field-cool (FC) susceptibilities show significant splitting below 180 K for $H \parallel c$, as shown in Fig. 3(a). Such irreversibility is a characteristic behavior of ferromagnetic compounds. The high-temperature susceptibility shows a weak anisotropy. On the other hand, χ_c ($H \parallel c$) is clearly higher than χ_{ab} ($H \parallel ab$), e.g., χ_c/χ_{ab} is about 13.8 at 200 K, indicating the anisotropic behavior in the order state. Furthermore, these results suggest that the easy magnetization direction should be parallel to the *c*-axis.

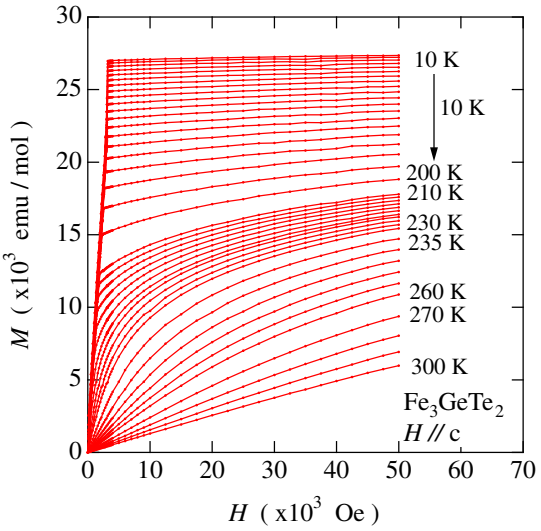

Fig. 4. (Color online) Isothermal magnetization curves for Fe_3GeTe_2 measured at various temperatures at magnetic field $H \parallel c$ of up to 5 T.

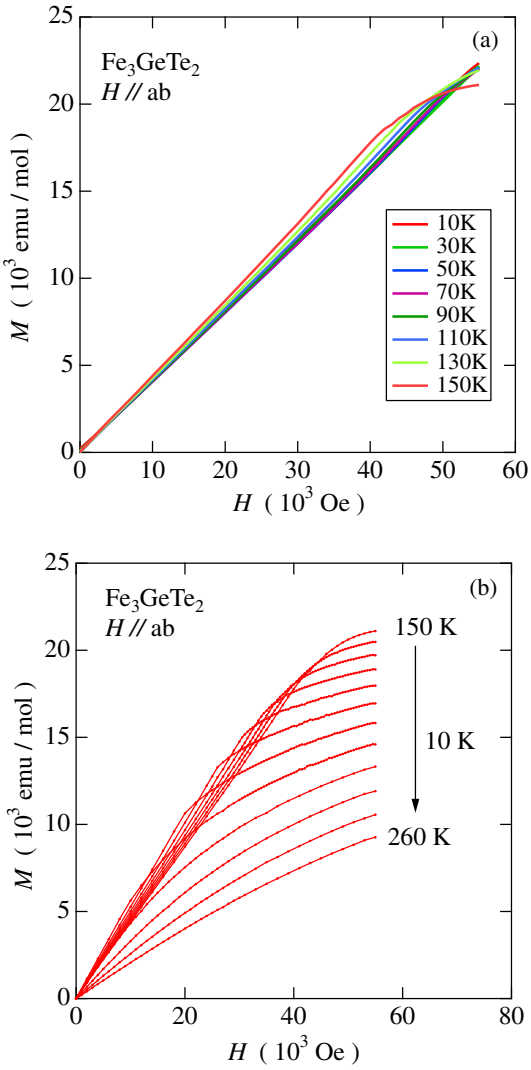

Fig. 5. (Color online) Isothermal magnetization curves for Fe_3GeTe_2 measured at various temperatures in magnetic field $H \parallel ab$-plane of up to 5.5 T. For clarity, M–H curves for $H \parallel ab$ with $T < 150$ K and $T > 150$ K are plotted in (a) and (b), respectively.

Figure 3(b) shows the corresponding T-dependence of the inverse susceptibility $1/\chi$. Excellent fitting to the data in the high-temperature range was obtained using the modified Curie–Weiss law

$$\chi = \frac{C}{T-\theta} + \chi_0, \tag{1}$$

where χ_0 is the temperature-independent susceptibility, C is the Curie–Weiss constant, and θ is the Weissa temperature. The values of the parameters obtained from the fitting are $C = 12.798$ (12.024) emu K/mol, $\theta = 204.97$ (225.71) K, and $\chi_0 = -0.026$ (-0.025) emu/mol for $H \parallel ab$ and $H \parallel c$. These results indicate that, at a high T, $\chi(T)$ shows a nearly isotropic paramagnetic behavior. From the fitting parameter, we deduced that the effective moment $P_{\text{eff}} = 4.7\,\mu_B$/Fe. A positive θ suggests that the ferromagnetic interaction among Fe atoms is dominant between the layers.

Figures 4 and 5 show the isothermal magnetization curves measured for Fe_3GeTe_2 in the temperature range from 10 to 300 K with $H \parallel c$ and $H \parallel ab$, respectively. The large anisotropic magnetic properties can be found in the ordered state. For the $H \parallel c$ shown in Fig. 4, M shows a saturation behavior at a very low H of about 3300 Oe. The same behavior is observed in the typical itinerant ferromagnet MnSi that shows a saturation behavior at about 6.2 kOe with $T = 4.2$ K.[14] With increasing temperature, the saturating magnetization decreases continuously, and M becomes proportional to H above 280 K. On the other hand, no saturation behavior but only a concave is observed for $H \parallel ab$. For clarity, the M–H curves for $H \parallel ab$ with $T < 150$ K and $T > 150$ K are plotted in Figs. 5(a) and 5(b), respectively. Note that a saturation tendency can be found at $H \sim 5$ T for the M–H curve measured with $H \parallel ab$ at 10 K as shown in Fig. 5(a). Higher H measurements are desired to confirm this saturation behavior.

On the basis of the mean-field theory, the Arrott plot (M^2–H/M) should be a straight line with an intercept that tends to zero as T approaches T_C. Therefore, one can derive the ferromagnetic transition temperature T_C accurately from the Arrott plot. The feasibility of this method has been confirmed in some materials, such as $Y(Co_{1-x}Al_x)_2$,[15–17] $ZrZn_2$,[18] Sc_3In,[19] and Ni_3Al.[20–22] Figure 6 shows the M^2 vs H/M plots at various temperatures for $H \parallel c$. M^2 does not show a linear relation but a curvature against H/M at all temperatures, particularly at approximately 220 K. This type of behavior has been observed in some materials, such as MnSi,[23] $Fe_xCo_{1-x}Si$,[24] and LaCoAsO.[4] In such cases, the M^4 vs H/M plot is very useful in determining T_C, as has been confirmed in these materials. Thus, we replotted the isothermal magnetization curves in the form of M^4 vs H/M, as shown in Fig. 7. Clearly, M^4 obeys the linear relation against H/M at approximately 220 K very well.

The linear relationship between M^4–H/M can be explained by the Takahashi theory, where the field effect of the critical thermal amplitude of spin fluctuations is taken into account. From the M^4–H/M plot, we determined T_C as the temperature at which the intercept along the M^4 axis crosses the origin of the coordinate axis. T_C is determined to be 220 K for Fe_3GeTe_2 which is slightly smaller than that reported in Ref. 11 (230 K).

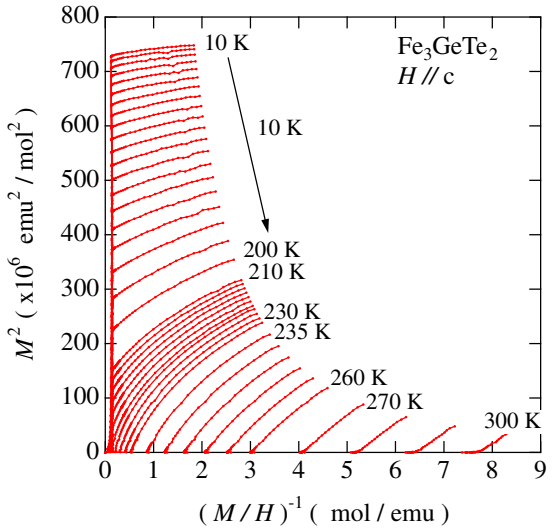

Fig. 6. (Color online) M^2 vs H/M plots (Arrott plot) for Fe_3GeTe_2 at various temperatures with $H \parallel c$.

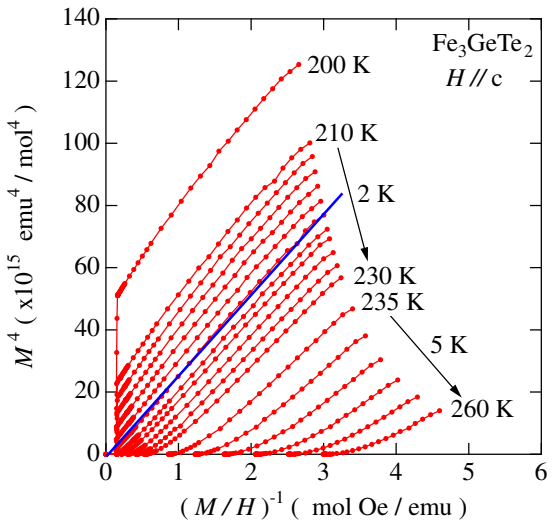

Fig. 7. (Color online) M^4 vs H/M plots for Fe_3GeTe_2 at various temperatures with $H \parallel c$. At approximately T_C, M^4 almost obeys the linear relation against H/M.

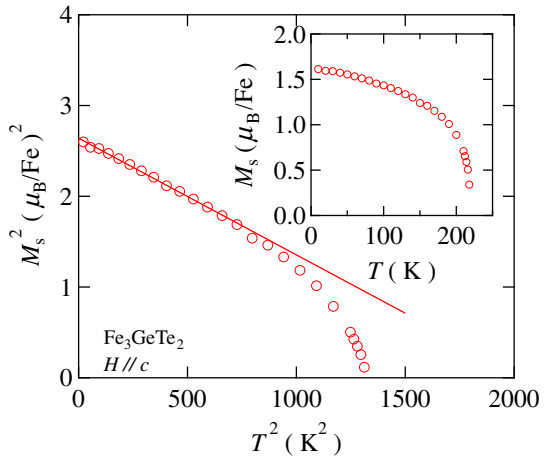

Fig. 8. (Color online) M_s^2–T^2 plot for Fe_3GeTe_2. The inset gives the corresponding M_s–T plot.

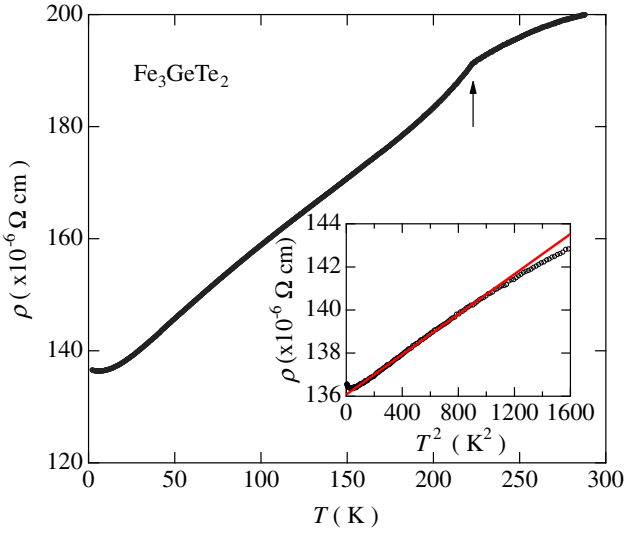

Fig. 9. (Color online) Temperature dependence of electrical resistivity of the single crystal of Fe_3GeTe_2 with current parallel to the *ab*-plane in the temperature range from 2 to 300 K. The arrow indicates the magnetic transition temperature. The inset shows the fit of the low-temperature resistivity data of Fe_3GeTe_2 with $\rho = \rho_0 + AT^2$.

Furthermore, we estimate the spontaneous magnetization $M_s(T)$ below T_C from Figs. 6 and 7. M_s is estimated as the value of the intersection of the extrapolation of the M^2 (M^4) curves with the vertical axis. The M_s value estimated from the M^2 and M^4 curves are almost the same below 150 K, so we only show those estimated from the M^2 curves in this temperature range. The M_s values between 160 and 220 K are estimated from the M^4–H/M plot. The obtained temperature dependence of M_s is shown in the inset of Fig. 8. From the value of the intersection of the natural extrapolation of the M_s curve with the vertical axis, we obtain the spontaneous magnetization $P_s = 1.625\,\mu_B$/Fe. This value is slightly larger than that previously reported ($1.20\,\mu_B$/Fe).[11] On the other hand, $T_C = 220$ K, can be considered as the temperature at which M_s decreases to zero with an increase in temperature. This value is consistent with the T_C determined from the M^4–H/M plot.

3.3 *Electrical resistivity*

Figure 9 shows the temperature dependence of the electrical resistivity $\rho(T)$ of the single crystal of Fe_3GeTe_2 with current parallel to the *ab*-plane in the temperature range from 2 to 300 K. The continuous decrease in $\rho(T)$ with decreasing temperature suggests the metallic behavior of the compound. The clear anomaly found at $T = 220$ K indicates the ferromagnetic phase transition, which is consistent with the magnetic measurements. The temperature dependence of resistivity at a low temperature can be well fitted with the power law, $\rho = \rho_0 + AT^2$ shown in the inset of Fig. 9. We obtained $\rho_0 = 136.1\,\mu\Omega\,\text{cm}$ and $A = 4.66 \times 10^{-9}\,\mu\Omega/\text{K}^2$.

3.4 *Heat capacity*

The temperature dependence of the heat capacity C_P for Fe_3GeTe_2 is shown Fig. 10. A clear jump corresponding to the ferromagnetic transition was observed at 220 K, which is

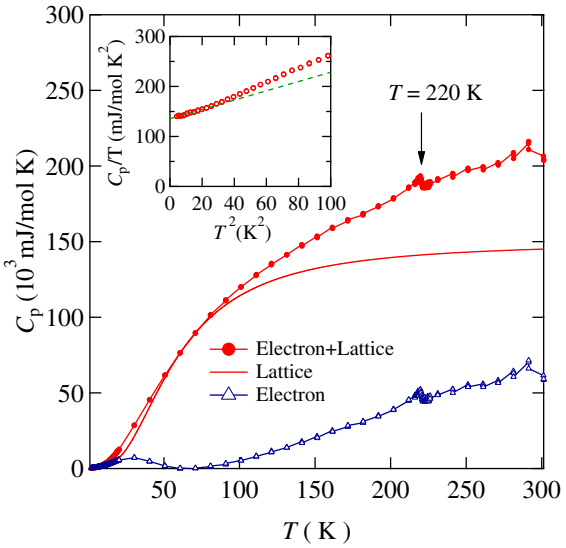

Fig. 10. (Color online) Heat capacity C_P vs temperature T for single crystal of Fe_3GeTe_2 between 2 and 300 K. The arrow shows the magnetic phase transition temperature T_C. The solid line and triangle indicate the lattice and electron contributions to C_P. The inset shows the $C_P(T)/T$ vs T^2 data below $T = 10$ K. The solid line through the data in the inset is a fit by the expression $C_P/T = \gamma + \beta T^2$.

consistent with the magnetic susceptibility and resistivity measurements. The C_P at room temperature is about 200 J/(mol K), which is larger than the Dulong Petit lattice heat capacity $C_P = 18R \cong 150$ J/(mol K) as expected for Fe_3GeTe_2; here, R is the molar gas constant. This may be due to the magnetic contribution in addition to the lattice contribution.

The inset of Fig. 10 gives the $C_P(T)/T$ vs T^2 plot for Fe_3GeTe_2 at low temperatures. For $T < 6$ K, the data can be well fitted by the expression

$$C_P(T)/T = \gamma + \beta T^2. \tag{2}$$

Here, the first term is the Sommerfeld electronic specific heat coefficient due to conduction electrons and the second term is the low-temperature limit of the lattice heat capacity. The resultant γ and β are 45.17 mJ/(Fe mol K^2) and 0.9291 mJ/(mol K^4), respectively. It is clearly that γ is strongly enhanced by spin fluctuations.

From β, one can estimate the Debye temperature using the expression

$$\theta_D = \left(\frac{12\pi^4 Rn}{5\beta}\right)^{1/3}, \tag{3}$$

where n is the number of atoms per formula unit ($n = 6$ for our compound). β yields $\theta_D = 232.36$ K. The calculated lattice contribution to C_P is shown in Fig. 10 by the solid line. Then, we can deduce the electron contribution to C_P as shown in Fig. 10 with triangles.

4. Discussion

Usually, the magnetic properties of itinerant materials can be understood in the framework of the Stoner model. However, this model excludes the spin fluctuation effect, leading to some problems remaining unsolved, such as the Curie temperature T_C and the Curie–Weiss behavior in the high temperature range. Moriya gave the SCR theory of spin fluctuations in order to take the spin fluctuation effect into account.[1)] Furthermore, Takahashi developed the theory by assuming that the sum of zero-point and thermal spin fluctuations is conserved against temperature; this gives a satisfactory explanation of the M^4 vs H/M plot, which has been observed in some magnetic materials.[2,23)]

Table I. Spin fluctuation parameters of Fe_3GeTe_2. T_0 was deduced from the SCR theory. T_A was obtained from the slope of the M^4–H/M plot at 220 K. $\bar{F}_1$ was estimated from the slope of the Arrott plot at 220 K. T_0^* and $\bar{F}_1{}^*$ were the best fitting parameters. Details can be found in the text.

T_C (K)	T_0 (K)	T_A (K)	$\bar{F}_1$ (K)	T_0^* (K)	$\bar{F}_1{}^*$ (K)
220	2298.77	795.8	96	1455	116

In the Takahashi theory of spin fluctuations, the relationship between M^4 and H/M is given by

$$M^4 = 1.17 \times 10^{18}\left(\frac{T_C^2}{T_A^3}\right)\left(\frac{H}{M}\right), \tag{4}$$

where M and H are in emu/mol and Oe units, respectively.[4)] The parameter T_A characterizes the dispersion of the spin fluctuation spectrum in wave vector space. Using the linear slope estimated from the M^4–H/M plot shown in Fig. 7 and $T_C = 220$ K for Fe_3GeTe_2, we obtained $T_A = 795.8$ K. On the other hand, T_A can also be deduced from the T^2-linear coefficient from the M_s^2–T^2 plot depending on this theory.[20,25,26)] From the linear fitting of the M_s^2–T^2 plot as shown in Fig. 8, we deduce $T_A = 111.8$ K, which is smaller than the value discussed above.

According to the SCR theory, T_C can be described as

$$T_C = (60c)^{-3/4} P_s^{3/2} T_A^{3/4} T_0^{1/4}, \tag{5}$$

where $c = 0.3353\cdots$, P_s is the spontaneous magnetization in μ_B unit, and T_0 characterizes the dispersion of the spin fluctuation spectrum in energy space. Using the values of T_C, P_s, and T_A estimated above, we obtained the characteristic temperature $T_0 = 2298.7$ K for Fe_3GeTe_2. All the parameters are summarized in Table I.

Furthermore, using the above parameters and the mode-mode coupling constant parameter $\bar{F}_1$, which is the coefficient of the M^4 term of the Landau expansion of free energy and can be determined from the slope of the Arrott plot ($\bar{F}_1$ for Fe_3GeTe_2 deduced from the Arrott plot is 96 K.), we can calculate the inverse magnetic susceptibility in the frame of the SCR theory for nearly ferromagnetic metals using[23,36)]

$$y = 1 + \eta K_0^2 \int_0^{1/K_0} dz\, z^3 \left[\ln u - \frac{1}{2u} - \Psi(u)\right], \tag{6}$$

where $y = \chi(0)/\chi$, $u = z(z^2 + y)/t$, $K_0^2 = 1/2\alpha T_A \chi(0)$, $\eta = 15\bar{F}_1 T_0/2(\alpha T_A)^2$, $t = T/T^*$, $T^* = T_0 K_0^3$, and $\Psi(u)$ is the digamma function.[36)] The calculated temperature dependence of the inverse magnetic susceptibility for Fe_3GeTe_2 is shown in Fig. 11 with a dashed line. The agreement between theoretical and experimental results is fairly good near T_C.

On the other hand, in order to modify the discrepancy in the high temperature range, we can also deduce T_0 with the experimental results T_A and $\bar{F}_1$ using

$$\bar{F}_1 = \frac{4k_B T_A^2}{15T_0}, \tag{7}$$

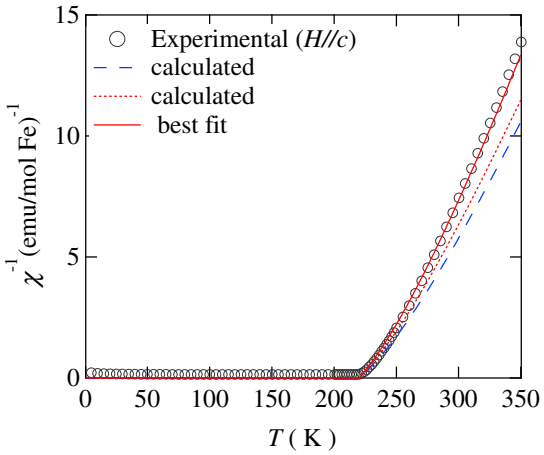

Fig. 11. (Color online) Temperature dependence of inverse susceptibility χ^{-1}. The dashed line represents the χ^{-1} calculated with T_0 determined on the basis of SCR theory. The dotted line indicates the χ^{-1} calculated with T_0 deduced using Eq. (7) on the basis of Takahashi theory of spin fluctuations. The solid line shows the best-fitted line for Fe_3GeTe_2.

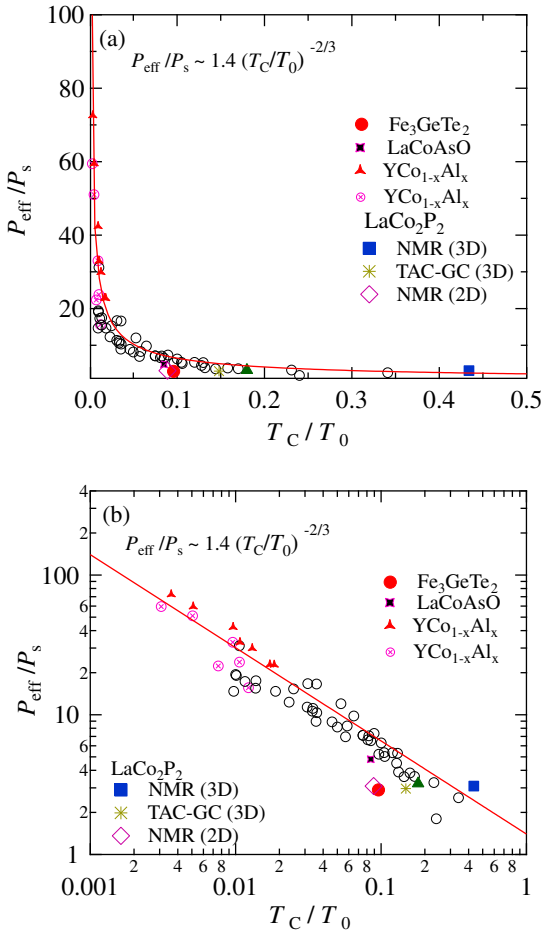

Fig. 12. (Color online) (a) Generalized Rhodes–Wohlfarth plot and (b) the corresponding log–log plot. The data for Fe_3GeTe_2 is plotted as a closed circle. The other plotted data are cited from Refs. 16 and 24, 28–35.

which can be deduced from the Takahashi theory of spin fluctuations.[2,23,25] The effectiveness of this formula has been confirmed by experiments.[3,20,25,37–39] The calculated value of T_0 is 1760 K. The calculated inverse susceptibility at $T_0 =$ 1760 K, T_A, and $\bar{F}_1$ is presented in Fig. 11 using a dotted line. Although the discrepancy is improved, unconformity still exists. Taking into account that $\bar{F}_1$ has a weak fitting temperature range dependence, we modify $\bar{F}_1$ and T_0 using Eq. (7), to obtain the best fitting of the inverse susceptibility. The best fitting parameters T_0^*, and $\bar{F}_1{}^*$ are indicated in Table I, and the corresponding fitting curve is shown in Fig. 11 by a solid line.

In order to clarify whether a magnetic material belongs to the itinerant or a localized spin system, the Rhodes–Wohlfarth ratio is a very good criterion in the Stoner model, which is defined as P_c/P_s, where $P_c(P_c+2) \equiv P_{eff}^2$ and P_s is the spontaneous magnetization in the ground state. In the case of a weak itinerant ferromagnet, the Rhodes–Wohlfarth ratio is much larger than that in the case of the localized spin system $P_c/P_s \equiv 1$. The rather large value of $P_c/P_s \equiv 3.8$ for Fe_3GeTe_2 indicates that the local moment description is inadequate.

More recently, a generalized Rhodes–Wohlfarth plot obtained on the basis of the SCR theory of spin fluctuations has been proposed by Takahashi. In this theory, the ratio T_C/T_0 is an important parameter as it characterizes the degree of localization or itineracy of the spin moment. At $T_C/T_0 \ll 1$, magnetic materials have a strong itinerant character, while at $T_C/T_0 \sim 1$, they exhibit local moment magnetism.[27] Taking the availability of M^4–H/M in this compound into account, we use the modified Rhodes–Wohlfarth plot to determine the degree of localization or itineracy of the spin moment in Fe_3GeTe_2. The estimated $T_C/T_0 = 0.096$ ($T_0 = 2298.7$ K is used here) for Fe_3GeTe_2, which is comparable to those reported for weak ferromagnets, such as MnSi (0.13), Ni_3Al (0.0116), and $ZrZn_2$ (0.053). When we plot P_{eff}/P_s and T_C/T_0 in the so-called Deguchi–Takahashi plot shown in Fig. 12(a),[15,24,28–35] the P_{eff}/P_s for Fe_3GeTe_2 is slightly smaller than the generalized Rhodes–Wohlfarth value $P_{eff}/P_s \sim 1.4(T_C/T_0)^{-2/3}$, as can be clearly seen in Fig. 12(b) in the log–log plot. This may be ascribed to the two-dimensionality of Fe_3GeTe_2, as has been pointed by Takahashi, where a smaller P_{eff}/P_s will be obtained with decreasing dimensionality from 3D to 2D for the same T_C/T_0.[2] Thus, we conclude that Fe_3GeTe_2 should be a quasi-2D itinerant ferromagnet.

5. Conclusions

We have successfully grown a single crystal of Fe_3GeTe_2 by the chemical transport method. The magnetic susceptibility, electrical resistivity, and heat capacity measurements of the crystal confirm the ferromagnetic transition at 220 K. The temperature dependence of magnetic susceptibility obeys the modified Curie–Weiss law quite well in the high-temperature range. The magnetization of Fe_3GeTe_2 by applying a magnetic field to the c-axis was found to show a convex curvature when plotted in an Arrott plot. The linear relation is obeyed in the M^4 vs H/M plot near T_C. By adopting the Takahashi theory, we estimated the spin fluctuation parameters T_A and T_0 to be about 795.8 and 2298.7 K, respectively, which can reproduce the inverse susceptibility χ^{-1} quite well. Furthermore, our results indicate that Fe_3GeTe_2 is a quasi-2D itinerant ferromagnet.

Acknowledgements

This work was supported by a Grant-in-Aid for the Global COE Program "International Center for Integrated Research and Advanced Education in Materials Science" and by Grants-in-Aid for Scientific Research (Nos. 19350030 and 22350029) from the Japan Society for the Promotion of Science.

*chenbinguanxin@hotmail.com
†kyhv@kuchem.kyoto-u.ac.jp

1) M. Hatatani and T. Moriya: J. Phys. Soc. Jpn. **64** (1995) 3434.
2) Y. Takahashi: J. Phys.: Condens. Matter **9** (1997) 10359.
3) S. Ikeda, Y. Maeno, and T. Fujita: Phys. Rev. B **57** (1998) 978.
4) H. Ohta and K. Yoshimura: Phys. Rev. B **79** (2009) 184407.
5) H. Ohta, C. Michioka, and K. Yoshimura: J. Phys. Soc. Jpn. **79** (2010) 054703.
6) H. Yanagi, R. Kawamura, T. Kamiya, Y. Kamihara, M. Hirano, T. Nakamura, H. Osawa, and H. Hosono: Phys. Rev. B **77** (2008) 224431.
7) A. S. Sefat, A. Huq, M. A. McGuire, R. Jin, B. C. Sales, D. Mandrus, L. M. D. Cranswick, P. W. Stephens, and K. H. Stone: Phys. Rev. B **78** (2008) 104505.
8) H. Sugawara, K. Ishida, Y. Nakai, H. Yanagi, T. Kamiya, Y. Kamihara, M. Hirano, and H. Hosono: J. Phys. Soc. Jpn. **78** (2009) 113705.
9) Y. Kamihara, T. Watanabe, M. Hirano, and H. Hosono: J. Am. Chem. Soc. **130** (2008) 3296.
10) N. Kh. Abrikosov, L. A. Bagaeva, L. D. Dudkin, L. I. Pertova, and V. M. Sokolova: Izv. Akad. SSSR, Neorg. Mater. **21** (1985) 1680.
11) H.-J. Deiseroth, K. Aleksandrov, C. Reiner, L. Kienle, and R. K. Kremer: Eur. J. Inorg. Chem. **2006** (2006) 1561.
12) A. C. Larson and R. B. Von Dreele: Los Alamos Nat. Lab. Rep. LAUR **86** (2000) 748.
13) B. H. Toby: J. Appl. Crystallogr. **34** (2001) 210.
14) C. Thessieu, K. Kamishima, T. Goto, and G. Lapertot: J. Phys. Soc. Jpn. **67** (1998) 3605.
15) K. Yoshimura, M. Mekata, M. Takigawa, Y. Takahashi, and H. Yasuoka: Phys. Rev. B **37** (1988) 3593.
16) K. Yoshimura, M. Takigawa, Y. Takahashi, H. Yasuoka, and Y. Nakamura: J. Phys. Soc. Jpn. **56** (1987) 1138.
17) K. Yoshimura and Y. Nakamura: Solid State Commun. **56** (1985) 767.
18) E. A. Yelland, S. J. C. Yates, O. Taylor, A. Griffiths, S. M. Hayden, and A. Carrington: Phys. Rev. B **72** (2005) 184436.
19) T. Hioki and Y. Masuda: J. Phys. Soc. Jpn. **43** (1977) 1200.
20) B. Chen, H. Ohta, C. Michioka, and K. Yoshimura: J. Phys. Soc. Jpn. **79** (2010) 064707.
21) B. Chen, C. Michioka, Y. Itoh, and K. Yoshimura: J. Phys. Soc. Jpn. **77** (2008) 103708.
22) J. Yang, B. Chen, H. Ohta, C. Michioka, K. Yoshimura, H. Wang, and M. Fang: Phys. Rev. B **83** (2011) 134433.
23) Y. Takahashi: J. Phys. Soc. Jpn. **55** (1986) 3553.
24) K. Shimizu, H. Maruyama, H. Yamazaki, and H. Watanabe: J. Phys. Soc. Jpn. **59** (1990) 305.
25) Y. Takahashi: J. Phys.: Condens. Matter **13** (2001) 6323.
26) K. Koyama, H. Sasaki, T. Kanomata, K. Watanabe, and M. Motokawa: J. Phys. Soc. Jpn. **72** (2003) 767.
27) K. Sato, T. Naka, M. Taguchi, T. Nakane, F. Ishikawa, Y. Yamada, Y. Takaesu, T. Nakama, A. de Visser, and A. Matsushita: Phys. Rev. B **82** (2010) 104408.
28) D. Bloch, J. Voiron, V. Jaccarino, and J. H. Wernick: Phys. Lett. A **51** (1975) 259.
29) F. R. de Boer, C. J. Schinkel, J. Biesterbos, and S. Proost: J. Appl. Phys. **40** (1969) 1049.
30) J. Takeuchi and Y. Masuda: J. Phys. Soc. Jpn. **46** (1979) 468.
31) S. Ogawa: J. Phys. Soc. Jpn. **40** (1976) 1007.
32) S. Ogawa: J. Phys. Soc. Jpn. **25** (1968) 109.
33) J. Beille, D. Bloch, and M. J. Besnus: J. Phys. F **4** (1974) 1275.
34) R. Nakabayashi, Y. Tazuke, and S. Murayama: J. Phys. Soc. Jpn. **61** (1992) 774.
35) A. Fujita, K. Fukamichi, H. Aruga-Katori, and T. Goto: J. Phys.: Condens. Matter **7** (1995) 401.
36) R. Konno and T. Moriya: J. Phys. Soc. Jpn. **56** (1987) 3270.
37) Y. Takahashi: J. Phys. Soc. Jpn. **79** (2010) 083707.
38) B. Chen, H. Ohta, C. Michioka, Y. Itoh, and K. Yoshimura: Phys. Rev. B **81** (2010) 134416.
39) J. Yang, B. Chen, H. Wang, Q. Mao, M. Imai, K. Yoshimura, and M. Fang: Phys. Rev. B **88** (2013) 064406.